行政院國家科學委員會專題研究計畫 成果報告

中間絲蛋白堆積導致神經元退化之研究(第 2 年)
研究成果報告(完整版)

計 畫 類 別 ：個別型
計 畫 編 號 ：NSC 97-2320-B-040-009-MY2
執 行 期 間 ：98 年 08 月 01 日至 99 年 07 月 31 日
執 行 單 位 ：中山醫學大學視光學系

計 畫 主 持 人：曾廣文

計畫參與人員：其他-兼任助理人員：張君妍

處 理 方 式 ：本計畫涉及專利或其他智慧財產權，2 年後可公開查詢

中 華 民 國 99 年 10 月 29 日

Autonomic Denervation in Mice with a Mutation in *Bullous Pemphigoid Antigen 1* (*BPAG1*) gene: An *in vivo* and *in vitro* study

Abstract

Dystonia musculorum (*dt*) is an autosomal recessive hereditary neuropathy that causes characteristic uncoordinated movement and is caused by a defect in the *bullous pemphigoid antigen 1* (*BPAG1*) gene. The neural isoform of *BPAG1* is expressed in various neurons, including in those the central and peripheral nerve systems of mice. However, most previous studies on neuronal degeneration in *BPAG1*-deficiency mice were focused on peripheral sensory neurons; limited investigation of the autonomic system has been conducted. To investigate the degeneration of autonomic peripheral nerves, patterns of nerve innervation in foot pads and irises from *dt/dt* mice were observed. Nerve innervation was assayed using general neuronal marker protein gene product 9.5 (PGP 9.5) via immunohistochemistry. Our results indicate not only peripheral sensory nerves but also autonomic innervation of sweats gland and irises dominated degeneration in *dt/dt* mice. Semi-quantitative results confirmed the numbers of neurons were significantly decreased in the sympathetic ganglia as well as parasympathetic ciliary ganglia of *dt/dt* mice compared to in both ganglia of wild-type mice. In addition, autonomic neurons were cultured from embryonic *dt/dt* mutants to elucidate degenerative patterns *in vitro*. We also found that the neuronal intermediate filaments (IFs) abnormally aggregated in cultured neurons from *dt/dt* embryos which

has been suggested that triggered the neuronal death in *dt/dt* mice *in vivo*. In conclusion, autonomic degeneration proceeds with diffuse innervation in foot pads and irises, and with a fewer neurons in autonomic ganglia of *dt/dt* mice. Furthermore, neuronal IFs aggregated in the juxtainuclear region of the cytoplasma could be detected in cultured neurons from the autonomic ganglia of *dt/dt* embryos. These results suggest that a deficiency in the cytoskeletal linker BPAG1 is responsible for not only dominant sensory nerve degeneration but also severe autonomic degeneration in *dt/dt* mice.

Key words: intermediate filament, nerve degeneration, autonomic ganglia, *dt/dt* mutant

Introduction

Dystonia musculorum (dt), an autosomal recessive hereditary neuropathy of the mouse, involving the ablative *bullous pemphigoid antigen 1* (*BPAG1*) gene (1). The human homology of a mouse sequence from the *Dystonia musculorum* locus is on chromosome 6p12 (2). Heterozygous *dt* mice seem normal phenotypically, but homozygous *dt* mice develop dystonia. Young *dt/dt* mutants are typically smaller than their normal littermates, and approximately two weeks after birth they exhibit abnormal postures and progressive loss of movement coordination. Hyperflexion and pronation in the foot paws are other symptoms (3). Previous studies have demonstrated not only substantial degenerative alterations, including in peripheral and central sensory pathways, but also slightly affected spinal motor neurons. This pathology appears to be primarily related to abnormal axonal accumulations of cytoskeleton in *dt/dt* mice (4, 5, 6, 7).

The cytoskeletal interacting protein, BPAG1, appears in several isoforms in different tissues (8). The neural isoform of BPAG1 mRNA, *BPAG1n*, has been detected in a variety of neuronal systems during normal growth, such as in neurons within dorsal root ganglia, trigeminal ganglia, sympathetic ganglia, enteric nerve system and spinal ventral horns (5). *BPAG1n* is generally expressed in neurons in numerous regions in wild-type mice, but not all neurons that are deficient in *BPAG1* cause serious degeneration in *dt/dt* mice. Most previous studies on neuronal degeneration in *dt/dt* mice were focused on the sensory nerve system. Investigations

have shown that the cytoskeletal interacting protein, BPAG1n, interacts with microtubules, microfilaments and neuronal IFs, has an important role in maintaining cytoarchitectural integrity (1, 8, 9, 10, 11).

Pathological change in *dt/dt* axonal degeneration has been found together with aggregation of IFs (4, 6). Moreover, studies in transgenic mice and in transfected-stable cell lines in which neuronal IF is overexpressed have demonstrated abnormal IF accumulation in the degenerating neurons (12, 13). These results may also be significant to neuronal diseases, in which IF protein aggregation plays an important role in neuronal degeneration. Abnormal IF protein aggregations in the cytoplasm are critical because the hyperphosphorylation of cytoplasmic IFs may trigger the neuronal death (14, 15, 16). In clinical neuropathy, neurodegenerative disorders are morphologically represented by progressive neuronal degeneration and an associated typical cytoskeleton change (17, 18). In addition, degenerative neurons with neuronal cytoplasmic inclusions have been observed in neuronal intermediate filament inclusions disease (NIFID) (19).

Neuroscience researchers are greatly concerned with elucidating neuronal degeneration and apoptosis associated with human neurological diseases. Many examples of amyotrophic lateral sclerosis in animals (20) have emphasized the importance of related animal models. Accordingly, the neurological mutant, *dt/dt* mouse, can be adopted examine the genetic and neurological basis of human diseases, such diseases of the peripheral nerve degeneration. The combination of impaired

nociception and autonomic dysfunction, in which motor neurons or axons are relatively or completely spared, is characteristic of autosomal recessive autonomic neuropathy (21). An investigation of changes in the nerve innervation and the neuronal number within autonomic ganglia of *dt/dt* may clarify the pathophysiology of mutation.

In this study, cutaneous tissue with immunohistochemical analyses and autonomic neuronal counting were performed on *dt/dt* mice *in vivo*. Furthermore, to study the patterns of neuronal IFs in autonomic neurons of *dt/dt*, sympathetic ganglia neurons were collected and assayed *in vitro*. The patterns of neuronal IFs in cultured sympathetic ganglia neurons were thoroughly studied by immunocytochemistry and conventional electron microscopy.

Materials and Methods

Mice

B6C3Fe-*ala-Dstdt-J* mice, carrying a natural mutation in the *BPAG1* gene, were utilized for this study. The experimental mice were collected from the littermates of heterozygous breeding pairs, provided by Jackson Laboratories (Bar Harbor, MA). Care and treatment of animals were in accordance with standard laboratory animal protocols approved by the Animal Care Committee (Chung Shan Medical University). A total of 37 adult mice (10 *dt/dt*, 11 *dt/+* and 16 wild-type) were collected from littermates of nine heterozygous breeding pairs for the following studies.

Reverse Transcriptase-Polymerase Chain Reaction (RT-PCR) Assays

Mice were scarified by cervical dislocation after anesthesia with choral hydrate (400 mg/kg of body weight, intraperitoneally). Total RNA from the tissue samples was prepared using Trizol reagent, and converted to cDNA using a reverse primer and reverse transcriptase (Invitrogen Corp., Carlsbad, CA). To amplify the cDNA, this study used Taq DNA polymerase and PCR, consisting of 40 cycles at 94°C for 30 sec, 65°C for 30 sec and, 72°C for 1 min. Specific PCR primer sequences were prepared as follows: *BPAG1n* primers (5'-GAC GAG AAG TCG GTG ATA ACC TAT G-3' and 3'-CTG TTT GAG TAG GAC GGG CTT-5', producing a 511-bp fragment). The primers of *β-actin* applied as a positive control, were 5'-AAC CAT GAG GGA AAT CGY GCA C-3' and 3'-AGT CAA GGG AAT CGG CAG AAT G-5' (producing a 219

bp fragment).

Immunohistochemistry for nerve tissues in foot pads

Young adult mice (8 weeks old) were anesthetized and perfused with 4% paraformaldehyde. Tissue samples were collected and then cut on a freezing microtome. Floating sections were changed in phosphate-buffered saline (PBS) solution, incubated in 3.5 % hydrogen peroxide to eliminate endogenous peroxidase activity, and finally blocked using 5% normal goat serum and 0.5% Triton X-100 in PBS. Sections were incubated with the primary antibodies against neuronal marker proteins at 4°C for 16-24 hrs. These antibodies against included a general neuronal protein such as protein gene product 9.5 (PGP 9.5, 1: 500, Chemicon, Temecula, CA). After rising in PBS, sections were incubated with biotinylated secondary antibody of appropriate specie (Sigma-Aldrich, ST. Louis, MO). The color reaction product was accomplished with a Vector ABC kit and with the DAB reaction (Vector Labs, Burlingame, CA).

Immunohistochemistry of nerve fibers in iris

To avoid the color reaction of DAB covered up by the pigment granule in the iris, the florescence immunohistochemistry technique was applied. Iridial wholemounts were labeled pan neuronal marker using florescence-labeled secondary antibody. Irises were incubated for 24 hours in the pan neuronal marker primary antibody (PGP 9.5,

Chemicon) at 4°C. After washing, tissues were then reacted for 2 hours with FITC-conjugated goat anti-rabbit IgG (Sigma-Aldrich), the flat-mount were analyzed with a Zeiss Axiophot microscope (Carl Zeiss, Oberkochen, Germany).

Quantifying Neuronal Number

To perform semi-quantitative analysis of the number of sympathetic neurons, lumbar ganglia were fully sectioned at 8 µm thickness. Every tenth section was subjected to examination to avoid double counting of cells and total 5-10 sections were selected for each ganglion. In this analysis, the results were expressed as a percentage of neuronal number in the sympathetic ganglion of wild-type mice, considered as 100%.

In ciliary ganglia, we adopted a different approach, given the small size of ganglia. Serial sections were stained with hematoxylin, and all neurons were counted throughout every section which covers the entire ciliary ganglia. Only those cells with distinct nuclei were counted to avoid double counting of cells.

Pupillary light reflex

Pupillary responses were measured in unanaesthetized age-matched 8 weeks old wild-type and *dt/dt* mice. Each animal was adapted to darkness for at least 30 min. Mice were placed ona custom-built stereotactic apparatus, by which animal movement was restricted by a 28mm diameter polyethylene tube. A beam of light was directed to the eye for evaluation of pupillary light reflex. The pupillary diameter was

measured and used to calculate pupil area.

Cell culture for embryonic neurons from sympathetic ganglia in wild-type and *dt/dt* mice

To determine the effect of neuronal IF in sympathetic neurons, sympathetic ganglia were dissected and collected from mouse embryos at the embryonic 15.5 day. To genotype each embryo from the heterozygous breeding, the spinal cord of each embryo was collected for RT-PCR analysis as in our previous study (6). Sympathetic ganglia collected from each embryo were treated with 0.25% trypsin without EDTA for 20 minutes at 37°C. Cells from sympathetic ganglia were physically dissociated by pipetting, plated in culture dishes (Corning, New York, NY), and then allowed to attach to coverslips plated with poly-D-lysine (Sigma-Aldrich). Culture medium was composed of Neurolbasal medium (Gibco, Grand Island, NY) supplemented with 20% FBS, 2% glucose, 2.5 mM L-glutamine, 2% B-27 and 100 ng/mL NGF (R&D Systems, Minneapolis, MN). Cultured sympathetic ganglia cells were collected at 5 day *in vitro* (DIV) for further analysis.

Electron microscopy for cultured neurons

Cultured cells were fixed with a fixative containing 4% paraformaldehyde and 1% glutaraldehyde in 0.1 M cacodylate buffer (pH 7.4). Tissues were dissected out and kept in the fixative overnight. Following post-fixation in 1% osmium tetroxide (OsO_4)

for 2 hrs, tissue samples were dehydrated through a graded series of ethanol, and then embedded in epon 812 resin. Ultrathin sections (70 nm-thick) were collected on copper grids, doubly stained with uranyl acetate and lead citrate, and observed under a Hitachi 7100 electron microscope (Hitachi, Tokyo, Japan).

Immunocytochemistry for cultured neurons from sympathetic ganglia

Embryonic neurons were cultured on poly-D-lysine coated glass coverslips in a cell culture dish. Cultured neurons were fixed in methanol for 30 min at 4°C and then permeabilized with 0.1% Triton X-100 in PBS for 5 min. After this, cells were incubated for 1 hour with primary antibodies against ubiquitin and medium-neurofilament (NF-M) (Sigma-Aldrich), followed by washing three times in PBS. Samples were then incubated with secondary antibodies and Hoechst 33342 (Sigma-Aldrich) at 27°C for 1 hr. Hoechst 33342 was applied to stain nuclei. Subsequently, cultured neurons were mounted and examined under a Zeiss LSM 510 META confocal spectral microscope.

Results

Genetic characterization of *dt/dt* Mice

This study first determined the expression patterns of *BPAG1n* mRNA from wild-type and *dt/dt* mice by RT-PCR. The *BPAG1n* mRNA could be detected in the dorsal root ganglia, sympathetic ganglia and ciliary ganglia of wild-type mice, but not in that of *dt/dt* mice (Fig. 1).

Sympathetic denervation in the sweat gland of *dt/dt* mice

To investigate sympathetic innervation, skin of the foot pad was immunoassayed using the antibody against PGP 9.5. In wild-type mice, various immunopositive nerves encircled the coiled tubules of sweat glands, forming an interlacing, dark and continuous pattern (Figs. 2A and 2B). In *dt/dt* mice, a few faintly stained immunopositive nerves were identified in the dermis of foot pads (Figs. 2C and 2D). In normal mice, numerous autonomic nerve encircled innervated sweat glands (Figs. 2E and 2F). However, sweat glands were significantly denervated, with only weak and disorganized immunoreactivity around them (Figs. 2G and 2H). From this observation, it could be implied that autonomic nerves that innervated sweat glands were poor in *dt/dt* (Table 1). Histopathological analysis revealed that sweat glands in *dt/dt* mutants were not significantly changed. The morphology of sweat glands in *dt/dt* mutants looks no difference as that in wild-type mice (Figs 2E and 2G).

Additionally, the morphology of lumbar sympathetic ganglia was investigated. Typical sympathetic neurons with visible nucleoli could be observed in wild-type mice (Figs. 2I and 2J). In *dt/dt* mice, the size of ganglion is smaller. Otherwise, the neuronal number was significantly reduced (Table 1 and Fig. 2K). More glial cells are easily identified in the ganglion of *dt/dt* mice (Fig. 2L).

The density of paraympathetic nerve significantly decrease in the iris of *dt/dt* mice

In irises, the wider diameter of pupil size could be noticeable in *dt/dt* mice. Dual autonomic innervation occurs in both sphincter and dilator muscle of the iris. In the wholemount iris of *dt/dt* mice, immunopositive fibers showed a marked decrease in density throughout the sphincter and dilator area compared with an intact control iris from wild-type (Figs. 3A and 3B).

Parasympathetic ciliary ganglion and short ciliary nerve run along the outer surface of the optic nerve in wild-type mice (Fig. 3C). However, the nerve bundle could be recognizable but fewer observed in *dt/dt* mice (Fig. 3D). To illustrate the relationship between the denervation and parasympathetic neuropathy of *dt/dt* mice, neurons in ciliary ganglia were also examined. The neuronal number was reduced and the size of neuron was significantly smaller in ciliary ganglia of *dt/dt* mice (Figs. 3E and 3F). These observations suggest that the parasympathetic innervation of irises is poor in *dt/dt* mice compared with that in wild-type mice (Table 1). To investigate the

functional defect of autonomic denervation in irises of *dt/dt* mice, the examination of light induced pupil reflex was applied. From functional test of the pupillary reflex, we observed the diameter of pupil size was notably wider and the iris constriction was weaker of pupil in response to light in *dt/dt* mice compared with that of wild-type mice (Figs. 3G and 3H).

Ultrastructural patterns of cultured sympathetic neurons from *dt/dt* embryos

In the cultured sympathetic neurons from *dt/dt* embryos at 5 DIV, massive accumulation of neuronal IFs could be observed in the cell processes (Figs. 4A and 4B). The density of IFs was very high and the pattern of IFs was randomly orientated. Some of entrapped organelles were also found in the swelling processes of cultured sympathetic neurons from *dt/dt* mutants (Fig 4A).

Morphological patterns of cultured sympathetic neurons were normal from wild-type mice (Fig. 5A). However, cultured neurons from *dt/dt* revealed prominent vacuolization, typical autophagosomal structures and condensed chromatin could be observed under light and electron microscopy (Figs. 5B-5E). Multi-membraned structures including late lysosomes and autophagosomes could be found in the cultured neurons which suggest that cells are trying to clean up the damaged organelles. Some cultured neurons with numbers vacuolization in cytoplasma of *dt/dt* exhibited the apoptotic-like death. The chromatin condensation with intact cell membrane could be observed in degenerative neurons from *dt/dt* (Figs. 5C and 5D).

Expression of ubiquitin in degenerating neuron with IFs accumulation

To determine the relationship between the IFs and the degrading proteins, NF-M and ubiquitin were examined by immunocytochemistry. At 5 DIV, cultured sympathetic neurons of wild-type mice displayed a rich expression of NF-M but not ubiquitin (Figs. 6A-6D). NF-M was normally distributed in axonal processes. However, two proteins of ubiquitin and NF-M were colocalized in various areas such as perikaryon in cultured sympathetic neurons from *dt/dt* mice (Figs. 6E-6H). The immunoreactivity indicated that the expression of ubiquitin protein was associated with the abnormal accumulation of neuronal IFs aggregations in degenerative sympathetic neurons from *dt/dt* mutants.

Discussion

Autonomic denervation in sweat glands and irises of *dt/dt* mice

Previous studies revealed that expression of *BPAG1-n* in variety of sensory and autonomic neurons from the embryonic to the postnatal stage in normal development, but morphometry study has been shown significant reduction limited in sensory innervations of *dt/dt* mutants (3, 5). This study indicates that not only the sensory nerve is markedly denervated in the cutaneous part of the foot pad, but also sympathetic innervation is severely impaired in the sweat gland of young adult *dt/dt* mice. The sympathetic innervated sweat glands substantially degenerated in foot pads of *dt/dt* mice. This degeneration was identified with immnunohistochemistry using general neuronal marker PGP9.5. Our new finding of the sympathetic denervation adds another criterion for phenotyping of *dt/dt* mice.

Ciliary ganglion, like sympathetic ganglion, is a neural crest-derived parasympathetic ganglion (22). The neuronal number of ciliary ganglion was significant decrease in *dt/dt* mice of this study. Moreover, our functional assay provide compelling evidence that the denervation of irises and the wider iridial diameter of pupillary response to light in *dt/dt* mice. Several facts of our investigations raised the prospect that BPAG1 gene has important role in normal development of the ciliary ganglion. The peripheral nerve system, including dorsal root ganglia, sympathetic ganglia and ciliary ganglia, develops from cells of the neural crest, which migrate during the embryonic stage (23). The loss of BPAG-n, a

cytoskeleton linker protein, in dorsal root ganglia and sympathetic ganglia neurons suggests that the cytoskeleton dysfunction may trigger the neuronal death during cell migration. This phenomenon may be responsible for the fact that of *BPAG1n* is expressed in numerous neurons during normal development, but in *BPAG1* deficiency mice neuronal degeneration is limited to peripheral neurons derived from neural crest cells.

The autonomic system is not considered to be affected by neurodegenerative disorders such as X-linked recessive spinobulbar muscular atrophy and Guillain-Barre syndrome, but observations have revealed autonomic skin denervation (24, 25). This investigation also demonstrated the sympathetic denervation of sweat glands in foot pads and parasympathetic denervation of irises in eyes from *dt/dt*. The terminal endings of the sympathetic nerve commonly degenerate more quickly than the proximal portion of the degenerating sympathetic ganglia neurons (26). In fact, skin innervation studies have established an early sign of neuropathy before ganglionopathy is detected (27). Cutaneous tissues and iridial wholemounts with immunohistochemical analysis constitutes a reliable approach for distinguishing between neuropathy and neuronopathy.

In this study, our data provided an evidence for epidermal and iridial denervation in foot pads and eyes with autonomic neuropathy in case of neuronal cytoskeletal dysfunction.

Roles of neuronal cytoskeletons in cultured sympathetic neurons from *dt/dt* embryos

Clinical and basic neuropathy has indicated that neurodegenerative disorders are morphologically represented by progressive neuronal damage, and are associated with the typical cytoskeleton dysfunction (12, 13, 17, 18). Other results have also indicated that abnormal aggregations of IF protein are significantly involved in the mechanism of neuronal death (19, 28, 29). In previous study of *dt/dt* mice, the abnormal accumulation of IFs in degenerating primary sensory neurons was observed *in vivo* and *in vitro* (6). It has also been established that the abnormal accumulation of neuronal IF proteins may impair axonal transport and later motivate the cascade of neuronal apoptosis of neurons in dorsal root ganglia of *dt/dt* (6). In our current study, abnormal translocation of neuronal IFs was found in the nerve process and soma of cultured sympathetic neurons from *dt/dt* embryos. It suggests that the deficiency in BPAG1, the cytoskeletons linker protein, may induce the process of neuronal death in the sympathetic nervous system of *dt/dt* mice.

Protein degradation in degenerating neurons from *dt/dt* mutants

Intracellular protein degradation is mediated mainly by the ubiquitin-proteasome and autophagy-lysosome systems in eukaryotic cells (30, 31). Ubiquitin-proteasome is chiefly responsible for degrading short-lived proteins and a selective form of catabolism (30). Repetition of the cycle generates polyubiquitin

chains on target proteins that are then degraded by the ubiquitin to smaller peptides. In contrast, autophagy is a broad term for the degradation of long-lived proteins and a nonselective form of catabolism (31). Some studies have revealed that abnormal protein aggregations, which are potential toxins, could be quickly degraded by the ubiquitin-proteasome and autophagy-lysosome systems (32, 33). Our immunomicroscopy images showed the involvement of ubiquitin in the degeneration neurons from *dt/dt*. In addition, preliminary transmission electron microscopy images reveal lysosomal or autophagosomal structures and pronounced vacuolization in the cultured sympathetic neurons. From our observation, we suggest that ubiquitin-proteasome or autophagy-lysosome systems may have essential roles in degrading neuronal IFs aggregations during the cell survival of sympathetic neurons in *dt/dt.*

In conclusion, we have demonstrated the epidermal denervation associated with sensory or autonomic neuropathy in this study of *dt/dt* mutants. Additionally, it has been shown that ubiquitin-proteasome and autophagy-lysosome systems may participate in the cell survival of cultured sympathetic neurons from *dt/dt* mutants.

Acknowledgements

The authors would like to thank the National Science Council of the Republic of China, Taiwan, for financially supporting this research under Grant No. NSC

97-2320-B-040-009-MY2 to K.W Tseng and NSC 97-2628-B-002-043-MY3 to C.L Chien.

References

1. Brown A, Bernier G, Mathieu M, Rossant J, Kothary R. 1995. The mouse dystonia musculorum gene is a neural isoform of bullous pemphigoid antigen 1. Nat Genet 10:301-306.

2. Brown A, Lemieux N, Rossant J, Kothary R. 1994. Human homolog of a mouse sequence from the dystonia musculorum locus is on chromosome 6p12. Mamm Genome 5: 434-437.

3. Duchen LW, Strich SJ, Falconer DS. 1964. Clinal and pathological studies of an hereditary neuropathy in mice (Dystonia Musculorum). Brain 87:367-378.

4. Sotelo C, Guenet JL. 1988. Pathologic changes in the CNS of dystonia musculorum mutant mouse: an animal model for human spinocerebellar ataxia. Neuroscience 27:403-424.

5. Dowling J, Yang Y, Wollmann R, Reichardt LF, Fuchs E. 1997. Developmental expression of BPAG1-n: insights into the spastic ataxia and gross neurologic degeneration in dystonia musculorum mice. Dev Biol 187:131-142.

6. Tseng KW, Lu KS, Chien CL. 2006. A possible cellular mechanism of neuronal loss in the dorsal root ganglia of Dystonia musculorum (dt) mice. J Neuropathol Exp Neurol. 336-47.

7. Tseng KW, Chau YP, Yang MF, Lu KS, Chien CL. 2008. Abnormal cellular translocation of alpha-internexin in spinal motor neurons of Dystonia musculorum mice. J Comp Neurol. 507:1053-64.

8. Leung CL, Green KJ, Liem RK. 2002. Plakins: a family of versatile cytolinker proteins. Trends Cell Biol 12:37-45.

9. Yang Y, Dowling J, Yu QC, Kouklis P, Cleveland DW, Fuchs E. 1996. An essential cytoskeletal linker protein connecting actin microfilaments to intermediate filaments. Cell 86:655-665.

10. Leung CL, Sun D, Zheng M, Knowles DR, Liem RK. 1999. Microtubule actin cross-linking factor (MACF): a hybrid of dystonin and dystrophin that can interact with the actin and microtubule cytoskeletons. J Cell Biol 147: 1275-1286.

11. Sun D, Leung CL, Liem RK. 2001. Characterization of the microtubule binding domain of microtubule actin crosslinking factor (MACF): identification of a novel group of microtubule associated proteins. J Cell Sci 114:161-172.

12. Ching GY, Chien CL, Flores R, Liem RK. 1999. Overexpression of alpha-internexin causes abnormal neurofilamentous accumulations and motor coordination deficits in transgenic mice. J Neurosci 19:2974-2986.

13. Chien CL, Liu TC, Ho CL, Lu KS. 2005. Overexpression of neuronal intermediate filament protein alpha-internexin in PC12 cells. J Neurosci Res 80:693-706.

14. Nixon RA. 1993. The regulation of neurofilament protein dynamics by phosphorylation: clues to neurofibrillary pathobiology. Brain Pathol. 3:29-38.

15. Lariviere RC, Julien JP. 2004. Functions of intermediate filaments in neuronal development and disease. J Neurobiol. 58:131-148.

16. Pierozan P, Zamoner A, Soska AK, Silvestrin RB, Loureiro SO, Heimfarth L, Mello e Souza T, Wajner M, Pessoa-Pureur R. 2010. Acute intrastriatal administration of quinolinic acid provokes hyperphosphorylation of cytoskeletal intermediate filament proteins in astrocytes and neurons of rats. Exp Neurol.

224:188-96.

17. Jellinger KA, Bancher C. 1998. Neuropathology of Alzheimer's disease: a critical update. J Neural Transm Suppl 54:77-95.

18. Dickson TC, King CE, McCormack GH, Vickers JC. 1999. Neurochemical diversity of dystrophic neurites in the early and late stages of Alzheimer's disease. Exp Neurol 156:100-110.

19. Cairns NJ, Grossman M, Arnold SE, Burn DJ, Jaros E, Perry RH, Duyckaerts C, Stankoff B, Pillon B, Skullerud K, Cruz-Sanchez FF, Bigio EH, Mackenzie IR, Gearing M, Juncos JL, Glass JD, Yokoo H, Nakazato Y, Mosaheb S, Thorpe JR, Uryu K, Lee VM, Trojanowski JQ. 2004. Clinical and neuropathologic variation in neuronal intermediate filament inclusion disease. Neurology 63:1376-1384.

20. Turner BJ, Talbot K. Transgenics, toxicity and therapeutics in rodent models of mutant SOD1-mediated familial ALS. 2008. Prog Neurobiol. 85: 94-134.

21. Rotthier A, Baets J, De Vriendt E, Jacobs A, Auer-Grumbach M, Levy N, BonelloPalot N, Kilic SS, Weis J, Nascimento A, Swinkwls M, Kruyt MC, Jordanova A, De Jonghe P, Timmerman V. 2009. Genes for hereditary sensory and autonomic neuropathies: a genotype-phenotype correlation. Brain. 132: 2699-711.

22. Lee VM, Sechrist JW, Luetolf S, Bronner-Fraser M. 2003. Both neural crest and placode contribute to the ciliary ganglion and oculomotor nerve. Dev Biol. 263:176-90.

23. Weston, J. A. (1963). A radioautographic analysis of the migration and localization of trunk neural crest cells in the chick. Dev. Biol. 6,279 -310.

24. Pan CL, Tseng TJ, Lin YH, Chiang MC, Lin WM, Hsieh ST. Cutaneous innervation in Guillain-Barré syndrome: pathology and clinical correlations. 2003. Brain. 126: 386-97.

25. Manganelli F, Iodice V, Provitera V, Pisciotta C, Nolano M, Perretti A, Santoro L. 2007. Small-fiber involvement in spinobulbar muscular atrophy (Kennedy's disease). Muscle Nerve. 36: 816-20.

26. Mundinger TO, Mei Q, Taborsky GJ Jr. 2008. Impaired activation of celiac ganglion neurons in vivo after damage to their sympathetic nerve terminals. J Neurosci Res. 86:1981-93.

27. Lauria G, Sghirlanzoni A, Lombardi R, Pareyson D. 2001. Epidermal nerve fiber density in sensory ganglionopathies: clinical and neurophysiologic correlations. Muscle Nerve. 24: 1034-9.

28. Bigio EH, Lipton AM, White CL, III, Dickson DW, Hirano A. 2003. Frontotemporal and motor neurone degeneration with neurofilament inclusion bodies: additional evidence for overlap between FTD and ALS. Neuropathol Appl Neurobiol 29: 239-253.

29. Josephs KA, Holton JL, Rossor MN, Braendgaard H, Ozawa T, Fox NC, Petersen RC, Pearl GS, Ganguly M, Rosa P, Laursen H, Parisi JE, Waldemar G, Quinn NP, Dickson DW, Revesz T. 2003. Neurofilament inclusion body disease: a new

proteinopathy? Brain. 126: 2291-303.

30. Ciechanover A, Orian A, Schwartz AL. 2000. Ubiquitin-mediated proteolysis: biological regulation via destruction. Bioessays. 22: 442-51.

31. Ahlberg J, Marzella L, Glaumann H. 1982 Uptake and degradation of proteins by isolated rat liver lysosomes. Suggestion of a microautophagic pathway of proteolysis. Lab Invest. 47: 523-32.

32. Hershko A, Ciechanover, A. 1998. The ubiquitin system. Annu Rev Biochem 67: 425-479.

33. Yamamoto A, Cremona ML, Rothman JE. 2006. Autophagy-mediated clearance of huntingtin aggregates triggered by the insulin-signaling pathway. J Cell Biol. 172:719-31

Figure Legend

Figure 1. Reverse transcriptae-polymerase chain rection analysis of BPAG1n and β-actin mRNAs from wild-type and *dt/dt* mice.

Polymerase chain reaction application of BPAG1n and β-actin was carried out using the primers described in "Materials and Methods". RNA was extracted from tissues and cDNA was generated. BPAG1n mRNA could be detected in the dorsal root ganglia, sympathetic ganglia and ciliary ganglia of wild-type mice, but not in *dt/dt* mice. β-actin primers were used as a positive control.

Figure 2. Localization of sympathetic nerves around sweat glands and neurons in sympathetic ganglion from wild-type and *dt/dt* mice.

Serial sections of foot pads were stained with hematoxylin or antibody against PGP 9.5 in wild-type (A, B, E and F) and *dt/dt* mice (C, D, G and H). In normal mice skin, numerous PGP 9.5-immunoreactive autonomic fibers are visible in dermis (A and B). Conversely, only some autonomic nerves are identifiable in *dt/dt* mice (C and D). High-power photomicrographs reveal that autonomic nerves innervated sweat gland and display dense and strong PGP 9.5 immunoreactivity in normal skin (E and F), while only fragmented autonomic nerves could be found in *dt/dt* mice (G and H). From the observation of lumbar sympathetic ganglia, the larger diameter of ganglia and neurons could be recognizable of wild-type mice (I and J). However, the size of neurons looks smaller in *dt/dt* mice than that in wild-type mice (K and L). Scale bars = 40 μm in A-H; 100 μm in K-L.

Figure 3. Degeneration of nerves irises and notably wider of pupil on response to

the light in *dt/dt* mice.

Wholemount preparations of irises were stained by immuneflorence for pan neuronal marker GP 9.5 (A and B). In wild-type mice, positive fibers are distributed circumferentially to the pupillary ruff in sphincter pupillae (SP) area and run radially toward the pupil in dilator pupillae (DP) area (A). Compared with intact wild-type mice, a few remained immunopositive fibers showed a marked decrease in density throughout the sphincter and dilator area in *dt/dt* mice (B). Ciliary ganglion (CG) and short ciliary nerve (SCN) could be found along the outer surface of the optic nerve (ON) in wild-type mice (C). However, the small nerve bundle (arrow) and ganglion (arrowhead) could be observed in *dt/dt* mice (D). High-power photomicrographs revealed that the ganglion with typical morphology was observed in wild-type mice (E), while the ganglion with fewer number and smaller size of neurons could be found in *dt/dt* mice (E and F). To investigate the effect denervation of iris of *dt/dt* mice, the light induced pupil reflex was applied. Using the pupillary reflex test, the diameter of pupil size is narrow in wild-type mice (G). Yet it is notably wider and the iris constriction is weaker of pupil in response to light in *dt/dt* mice (H). Scale bars = 200 μm in A-F; 2mm in G, H.

Figure 4. Ultrastructural patterns of neuronal intermediate filaments (IFs) in degenerating cultured sympathetic neurons from *dt/dt* embryos.

On the ultrastructural level, IF aggregates and randomly orientated IFs could be observed in cultured sympathetic neurons from embryonic *dt/dt* mice (A). The neuronal IFs formed aggregates in soma that might be involved in the degeneration of neurons from *dt/dt* mice. The random orientation of IFs and axonal organelles is found in the swelling processes of sympathetic neurons from *dt/dt* embryos (B). Scale bars = 1 μm.

Figure 5. Cellular patterns of autophagic structures on cultured sympathetic neurons from *dt/dt* mice.

In semithin sections (A, B and C), the morphological patterns of cultured neurons are normal from wild-type mice (A). Yet some membrane-bounded vesicles in perikaryon (B, arrows) and chromatin condensation (C, arrowheads) could be found in cultured neurons of *dt/dt* mutants. At the ultrastructural level, images of cultured neurons reveal autophagic structures and prominent vacuolization from *dt/dt* mice. Furthermore, the apoptotic-like characteristic of chromatin condensation with intact nuclear envelope and cell membrane could be observed from *dt/dt* embryos (D). Multi-membraned autophagosomes could be found in the cytoplasm of *dt/dt* mutants (E). Scale bars = 50 μm in A, B, C; 1μm in D, E.

Figure 6. Immunoreactivity of ubiquitin and NF-M in cultured neurons from wild-type and *dt/dt* mice.

Cultured neurons were double-labeled with antibodies to ubiquitin (green) and NF-M (red) and their nuclei were stained with Hoechst 33342 (blue). Ubiquitin-positive cells were not found in neurons from wild-type (A-D). Cultured neurons with abnormal accumulations of NF-M were observed mostly in the proximal region of axons and within cell bodies of cultured sympathetic neurons from *dt/dt* mutants (F). A number of neurons with NF-M accumulations were also labeled with the antibody to the ubiquitin (E, F and H). Scale bars = 40μm.

Table 1. Semi-quantitative analysis (%) of nerve innervation and neurons in young adult *dt/dt* mice compared with wild-type mice of the same age.

	Region	Nerve innervation and neuronal number of *dt/dt* mice (Relative number to the wild-type)
Types of nerve	Sympathetic innervation of sweat glands	5.8 ± 1.7%*
	Parasympathetic innervation of irises	15. 6± 1.2%*
Types of neuron	Lumbar sympathetic ganglia	34.3±17.4%*
	Ciliary ganglia	42.8±16.2%*

The nerve innervation and neuronal number of ganglia were calculated from wild-type (n=5) and *dt/dt* (n=4) mice. Semi-quantitative analysis was expressed as a percentage of the nerve innervation and the neuronal number in ganglia of wild-type mice considered as100%. Results are expressed as mean ± SD and *indicates a statistically different value (*t*-test, $P<0.01$) from the wild-type control.

Figure 1

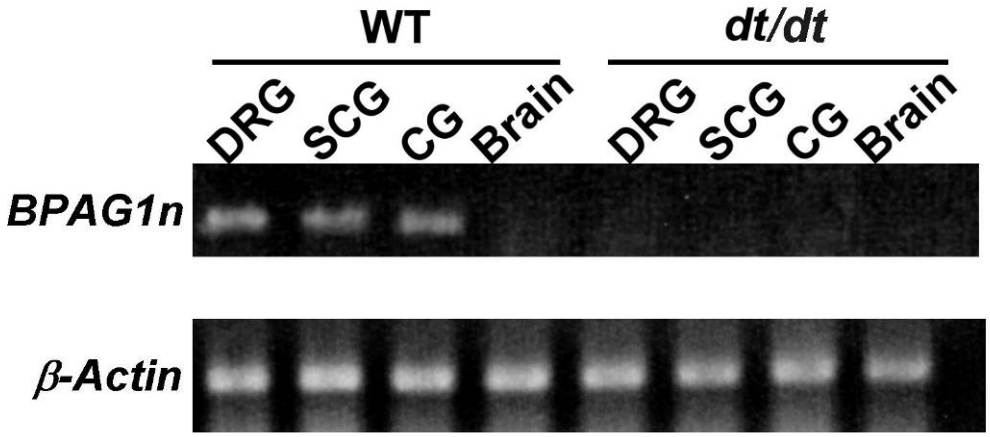

Figure 2

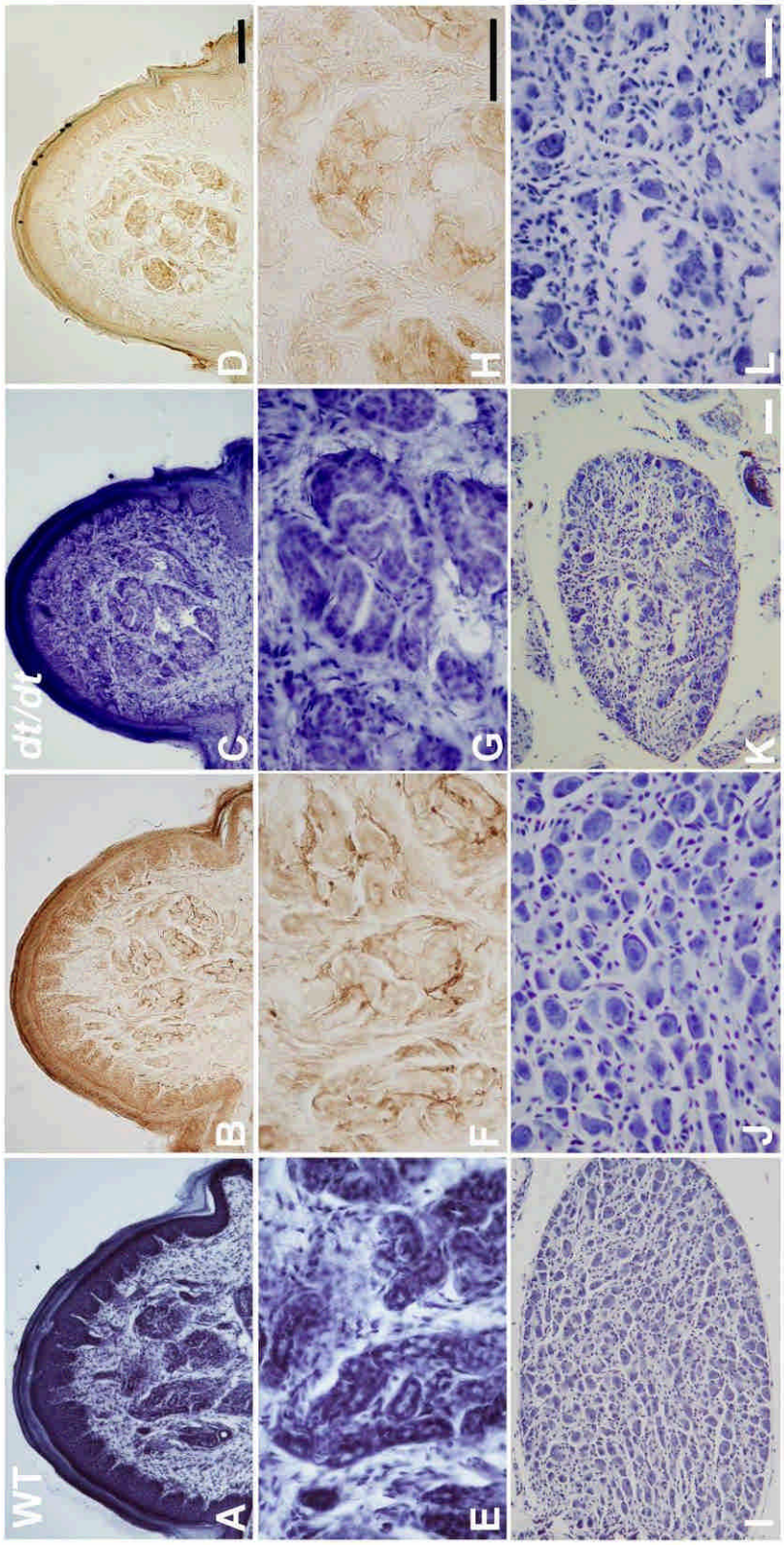

Figure 3

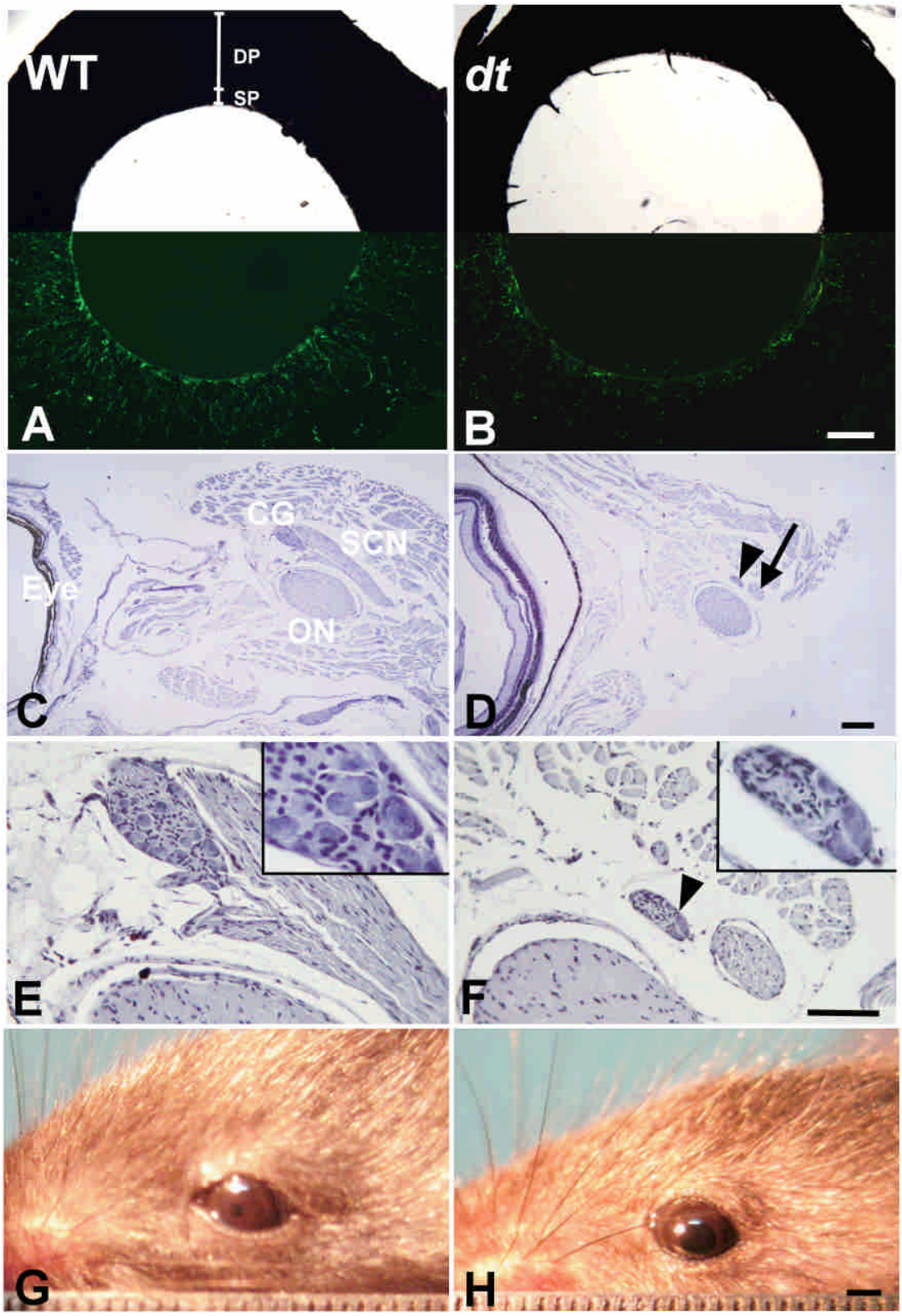

Figure 4

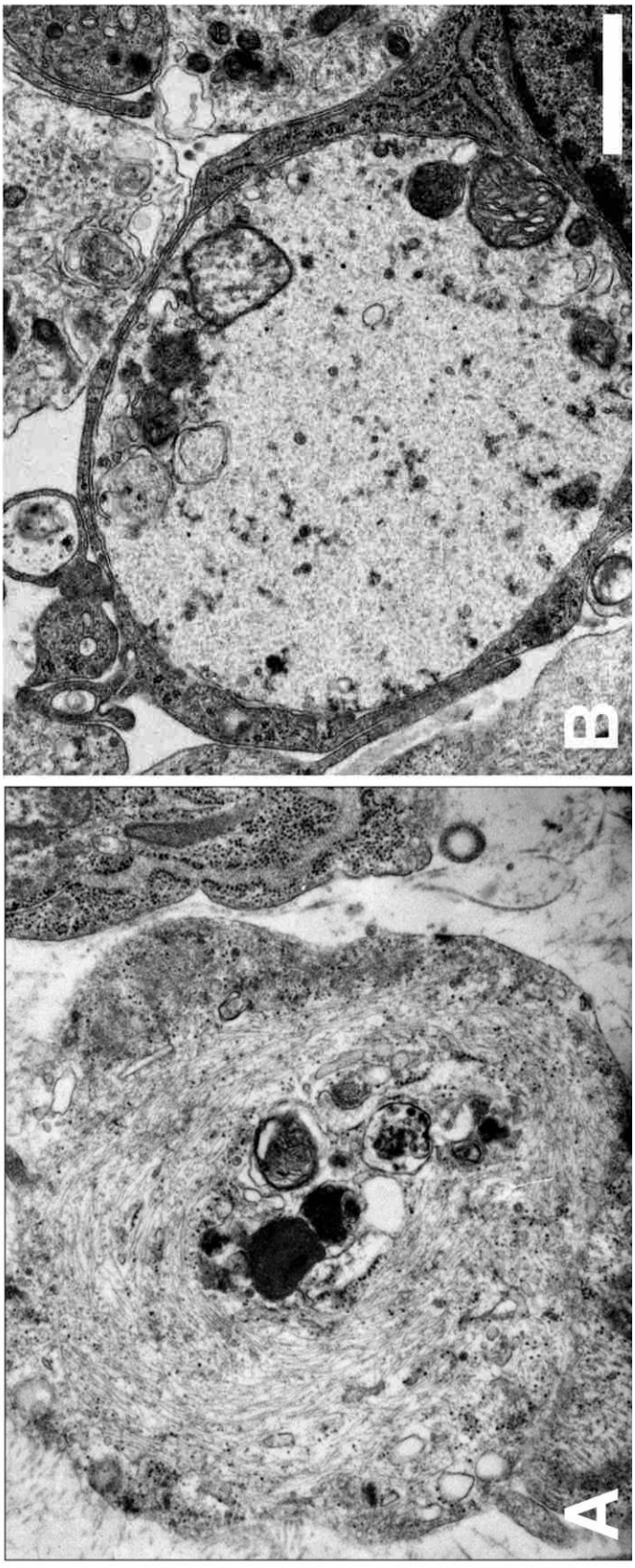

Figure 5

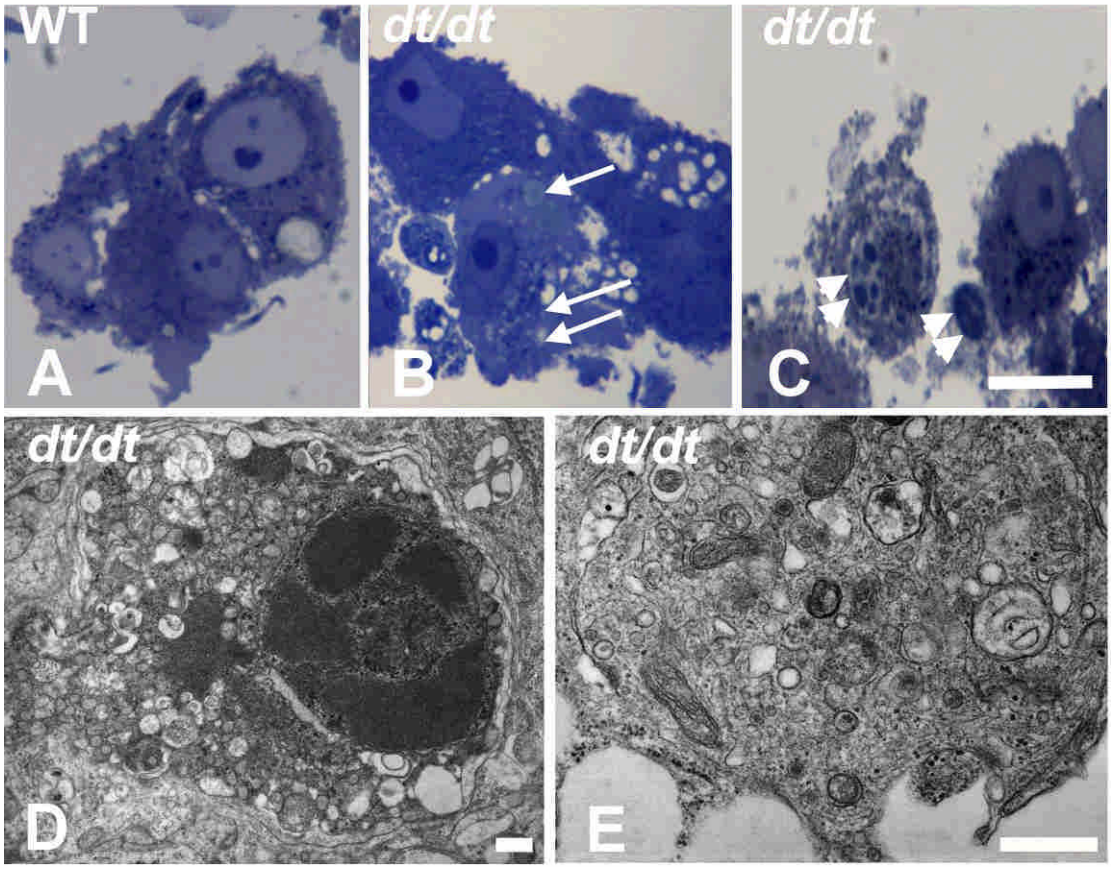

Figure 6

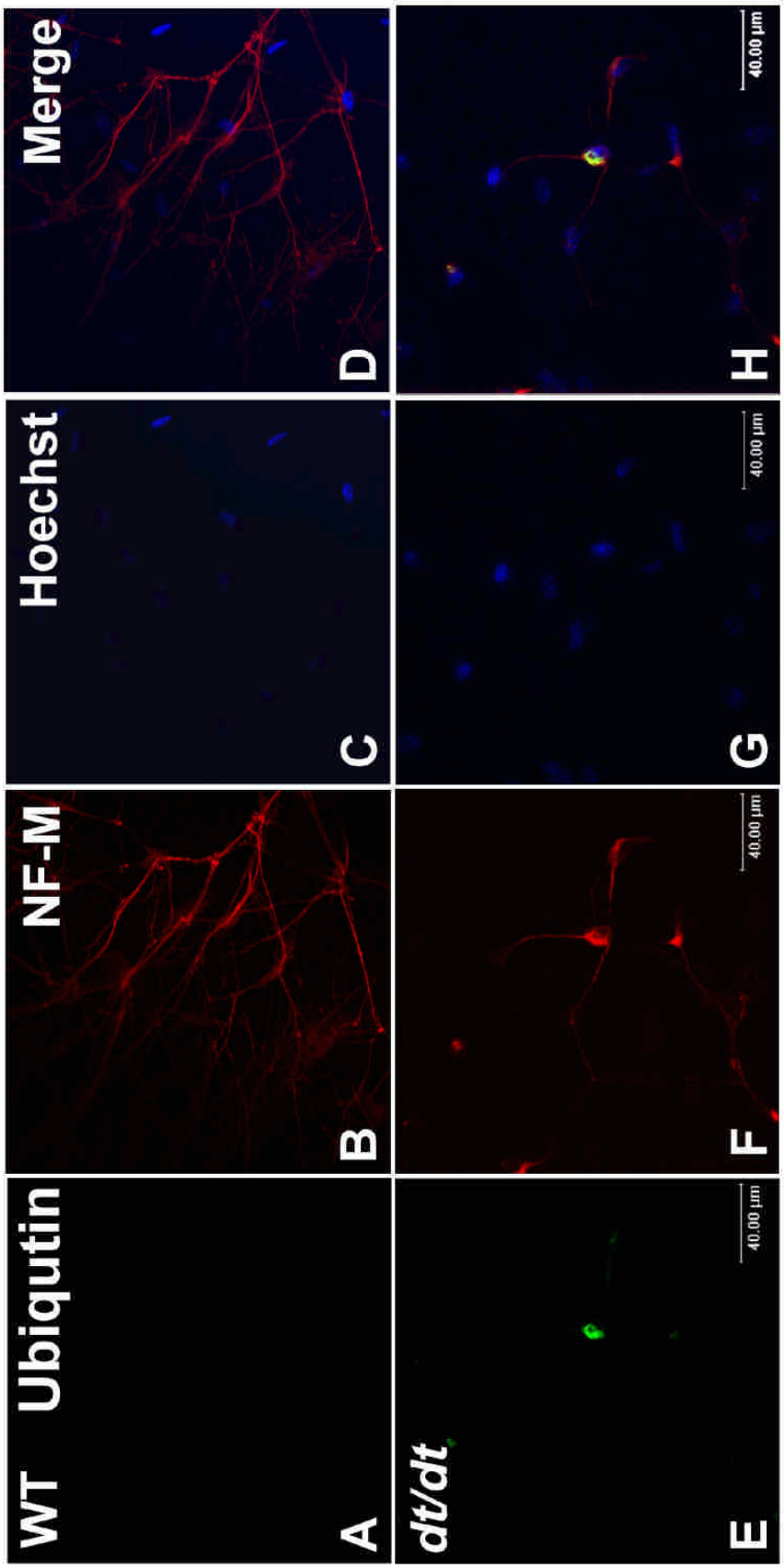

無衍生研發成果推廣資料

97 年度專題研究計畫研究成果彙整表

計畫主持人：曾廣文	計畫編號：97-2320-B-040-009-MY2
計畫名稱：中間絲蛋白堆積導致神經元退化之研究	

成果項目			量化			單位	備註（質化說明：如數個計畫共同成果、成果列為該期刊之封面故事...等）
			實際已達成數（被接受或已發表）	預期總達成數(含實際已達成數)	本計畫實際貢獻百分比		
國內	論文著作	期刊論文	1	1	100%	篇	Sensory and Sympathetic Denervation in the Foot Pads of Mice with a Defect in Bullous Pemphigoid Antigen 1(BPAG1) geneChung Shan Med J 21: 189-199, 2010
		研究報告/技術報告	0	0	100%		
		研討會論文	2	2	100%		
		專書	0	0	100%		
	專利	申請中件數	0	0	100%	件	
		已獲得件數	0	0	100%		
	技術移轉	件數	0	0	100%	件	
		權利金	0	0	100%	千元	
	參與計畫人力（本國籍）	碩士生	0	0	100%	人次	
		博士生	0	0	100%		
		博士後研究員	0	0	100%		
		專任助理	0	0	100%		
國外	論文著作	期刊論文	0	1	100%	篇	
		研究報告/技術報告	0	0	100%		
		研討會論文	0	0	100%		
		專書	0	0	100%	章/本	
	專利	申請中件數	0	0	100%	件	
		已獲得件數	0	0	100%		
	技術移轉	件數	0	0	100%	件	
		權利金	0	0	100%	千元	
	參與計畫人力（外國籍）	碩士生	0	0	100%	人次	
		博士生	0	0	100%		
		博士後研究員	0	0	100%		

		專任助理	0	0	100%		
其他成果 (無法以量化表達之成果如辦理學術活動、獲得獎項、重要國際合作、研究成果國際影響力及其他協助產業技術發展之具體效益事項等，請以文字敘述填列。)		本計劃完成之後，吾人能對中間絲蛋白的堆積，導致交感神經退化與凋亡的機制能提出新的見解；並利用持續表現 ubiquitin 細胞株的實驗模式，探討神經退化時，ubiquitin proteasome system 在神經元所扮演的保護性角色。					

	成果項目	量化	名稱或內容性質簡述
科教處計畫加填項目	測驗工具(含質性與量性)	0	
	課程/模組	0	
	電腦及網路系統或工具	0	
	教材	0	
	舉辦之活動/競賽	0	
	研討會/工作坊	0	
	電子報、網站	0	
	計畫成果推廣之參與（閱聽）人數	0	

國科會補助專題研究計畫成果報告自評表

請就研究內容與原計畫相符程度、達成預期目標情況、研究成果之學術或應用價值（簡要敘述成果所代表之意義、價值、影響或進一步發展之可能性）、是否適合在學術期刊發表或申請專利、主要發現或其他有關價值等，作一綜合評估。

1. 請就研究內容與原計畫相符程度、達成預期目標情況作一綜合評估

■達成目標

□未達成目標（請說明，以 100 字為限）

□實驗失敗

□因故實驗中斷

□其他原因

說明：

2. 研究成果在學術期刊發表或申請專利等情形：

論文：□已發表 ■未發表之文稿 □撰寫中 □無

專利：□已獲得 □申請中 ■無

技轉：□已技轉 □洽談中 ■無

其他：(以 100 字為限)

3. 請依學術成就、技術創新、社會影響等方面，評估研究成果之學術或應用價值（簡要敘述成果所代表之意義、價值、影響或進一步發展之可能性）(以 500 字為限)

在神經科學研究領域，探討神經細胞的退化與凋亡已成為今日生物醫學界的重要挑戰。本計劃以神經性缺陷的突變小鼠 Dystonia musculorum (dt) 做為生物研究材料，探討台灣常見的神經性疾病，例如老年癡呆症與肌萎縮性脊髓側索硬化症。臨床上，許多神經退化疾病都有的病理特徵，是會伴隨其細胞骨架排列的變化以及細胞骨架大量堆積於神經元。但造成神經元中間絲蛋白這種細胞骨架蛋白堆積的機制目前尚未完全釐清，可能因素包括:遭受毒物後的反應、神經元內不正常大量製造中間絲蛋白或神經纖維運輸障礙等原因。而在過往 dt 小鼠研究中也觀察到相同神經退化的病理特徵，神經元或神經軸突內均有中間絲蛋白堆積的現象。

本計劃完成之後，吾人能對中間絲蛋白的堆積，導致交感神經退化與凋亡的機制能提出新的見解;並利用持續表現 ubiquitin 細胞株的實驗模式,探討神經退化時,ubiquitin proteasome system 在神經元所扮演的保護性角色。